Available online at www.sciencedirect.com
ScienceDirect
International Journal of Heat and Mass Transfer 51 (2008) 4018–4024
International Journal of HEAT and MASS TRANSFER
www.elsevier.com/locate/ijhmt

Heat transfer over a bidirectional stretching sheet with variable thermal conditions

I-Chung Liu [a], Helge I. Andersson [b,*]

[a] Department of Civil Engineering, National Chi Nan University, 1 University Road, Puli, Nantou, Taiwan 545, ROC
[b] Department of Energy and Process Engineering, Norwegian University of Science and Technology, 7491 Trondheim, Norway

Received 4 May 2007; received in revised form 21 August 2007
Available online 20 February 2008

Abstract

The heat transfer characteristics of a steady three-dimensional viscous fluid flow driven by the bidirectional stretching of an elastic surface are investigated. The hydrodynamic part of the problem is determined by the ratio between the stretching rates in the two lateral directions. The prescribed temperature or heat transfer rate varies along the surface. A heat source is included in the thermal boundary layer equation, which transforms into an ordinary differential equation by means of a similarity transformation. The numerical results show that the principal effect of the variable surface conditions is to thicken the thermal boundary layer when the temperature or heat transfer rate decreases with the distance from the center of sheet. The boundary layer thickness is correspondingly reduced if the sheet temperature or heat transfer rate increases in one or both of the lateral directions.

Keywords: Thermal boundary layers; Stretched surfaces; Variable surface temperature; Variable surface heat flux; Internal heat generation

1. Introduction

The analysis of boundary layer flows of viscous fluids driven by a moving surface rather than by an external 'free stream' dates back to the pioneering investigation by Sakiadis [1]. He considered the steady two-dimensional boundary layer developing along a constantly moving flat plate. Even though the momentum boundary layer equation for the Sakiadis-problem is identical to the classical Blasius boundary layer equation, the different boundary conditions make the resulting similarity solutions rather different. This difference is brought about by the substantial entrainment of ambient fluid, which makes the Sakiadis boundary layer thicker than the Blasius boundary layer.

Surface-driven boundary layers are of practical importance for instance in extrusion processes. When a polymer sheet is drawn from a slit, the sheet is often being stretched. Since the sheet speed near the slit is low, the local sheet velocity can be approximated as a linear function of the distance from the slit. This fact probably motivated Crane [2] to investigate the viscous boundary layer flow along a linearly stretched elastic sheet, for which he derived an explicit analytical solution for the fluid motion. Since the mechanical properties of the final product depend crucially on the rate of cooling or heating along the surface while being stretched, Gupta and Gupta [3], Vleggaar [4] and Dutta et al. [5] examined the heat transfer characteristics of the boundary layer flow considered by Crane [2] for cases with constant wall temperature [3,4] and constant wall heat flux [5]. The former problem was subsequently extended by Carragher and Crane [6] and Grubka and Bobba [7] to boundary layer flow over linearly stretching sheets which exhibit a power-law variation of the sheet temperature.

The stretching of a filament or sheet imparts a unidirectional orientation on the elastic material, which in turn affects the mechanical properties of the resulting product. The previous studies [1–7] were all limited to two-dimensional boundary layer problems arising from a unidirectional

* Corresponding author. Tel.: +47 73 59 35 56; fax: +47 73 59 34 91.
E-mail address: helge.i.andersson@ntnu.no (H.I. Andersson).

0017-9310/$ - see front matter © 2007 Elsevier Ltd. All rights reserved.
doi:10.1016/j.ijheatmasstransfer.2007.10.041

Nomenclature

a, b	lateral stretching rates (s^{-1})
A, B	constants of proportionality
C	constant in Eq. (16)
c_p	specific heat at constant pressure
${}_1F_1$	confluent hypergeometric function
f', g'	dimensionless velocity components
m, n	dimensionless parameters in confluent hypergeometric function
Pr	Prandtl number, υ/κ
q	coefficient of volumetric heat source
r, s	power indices
T	dimensional temperature
u, v, w	dimensional velocity components
x, y, z	dimensional coordinates

Greek symbols

α	stretching ratio, b/a
β	dimensionless strength of source or sink, $q/\rho c_p a$
η	similarity variable, $(a/\upsilon)^{1/2}z$
θ	dimensionless temperature (PST)
κ	thermal diffusivity
λ	thermal conductivity,
μ	dynamic viscosity
υ	kinematic viscosity, μ/ρ
ρ	density
ϕ	dimensionless temperature (PHF)

Subscripts

w	wall value
∞	property at infinity

stretching. Wang [8], however, analyzed the three-dimensional flow of viscous fluids caused by the stretching of an elastic flat surface or membrane in two lateral dimensions. In the general case with different stretching rates in the two perpendicular directions, Wang [8] resorted to direct numerical integration of the resulting boundary value problem, whereas Ariel [9] more recently demonstrated that this problem also admits solutions in terms of series of exponentially decaying functions. In this bidirectional stretching sheet problem, the ratio α between the stretching rates in the two lateral directions becomes an essential parameter. While $\alpha = 1$ signifies axisymmetric stretching, Crane's two-dimensional case [2] is recovered in the limiting case $\alpha = 0$.

The thermal boundary layer problem accompanying Wang's hydromechanical problem [8] was investigated by Laha et al. [10] both for uniform surface temperature and uniform surface heat flux. For the isothermal sheet, they observed that, for given Prandtl number Pr, the temperature at a point decreased with increase in the stretching ratio α. Similarly, for fixed Pr, the magnitude of the excess sheet temperature over the ambient temperature decreased with increasing α for a given uniform heat flux.

In practical situations, the thermal characteristics may vary along the sheet, for instance as considered by Carragher and Crane [6] and Grubka and Bobba [7] in the two-dimensional case, i.e. unidirectional stretching. The purpose of the work reported in the present paper is to examine the heat transfer characteristics associated with the three-dimensional hydrodynamical flow considered by Wang [8] and Ariel [9] with either prescribed variable surface temperature (PST) or prescribed variable surface heat flux (PHF). The present analysis also includes the presence of a temperature-dependent internal heat source (or sink), which was not taken into account by Laha et al. [10].

2. Problem formulation

We consider the three-dimensional steady boundary layer flow of a viscous incompressible fluid driven by an elastic flat surface in the plane at $z = 0$, as shown in Fig. 1. The surface is stretched uniformly in both horizontal directions such that the surface velocity components are ax and by in the x- and y-directions, respectively. Here, a and b are the two constant stretching rates, both being positive and with dimension time^{-1}. This three-dimensional flow problem, which results from the bidirectional stretching, is rather different from the two-dimensional momentum boundary layer problem formulated by Sakiadis [1] for flow driven by a continuously moving sheet emerging from a slit at $x = 0$.

The bidirectional stretching sheet problem was first formulated by Wang [8] who introduced a similarity transformation to recast the governing partial differential equations into a set of ordinary differential equations (ODEs). Following Wang [8], the three velocity components (u, v, w) in the Cartesian coordinate system are transformed according to

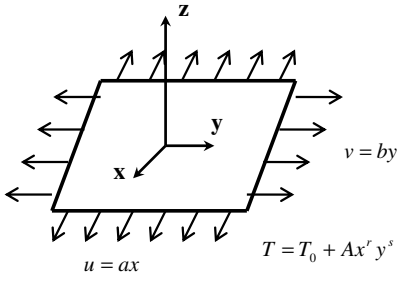

Fig. 1. Physical configuration and coordinate system.

$$u = axf'(\eta), \quad v = ayg'(\eta), \quad w = -(a\upsilon)^{1/2}(f+g), \tag{1}$$

where $\eta = (a/\upsilon)^{1/2} z$ is the similarity variable and υ is the kinematic viscosity of the fluid. The continuity equation is, of course, satisfied by Eq. (1), provided that the minus sign is included in the transformation of the velocity component w perpendicular to the sheet. This minus sign, which implies that the ambient fluid is driven *towards* sheet, is absent in the papers by Wang [8] and Ariel [9]. The appropriate boundary conditions for the velocity components are

$$u = ax, \quad v = by, \quad w = 0 \text{ at } z = 0 \tag{2}$$

and

$$u \to 0, v \to 0 \text{ as } z \to \infty \tag{3}$$

at the sheet $z = 0$ and outside the momentum boundary layer, respectively.

After substituting the transformation (1) into the momentum boundary layer equations and boundary conditions, we obtain

$$f''' + (f+g)f'' - f'^2 = 0 \tag{4}$$

$$g''' + (f+g)g'' - g'^2 = 0 \tag{5}$$

and

$$f(0) + g(0) = 0, f'(0) = 1, g'(0) = b/a \equiv \alpha,$$
$$f'(\infty) = 0, g'(\infty) = 0, \tag{6}$$

where the primes denote differentiation with respect to η and α is the stretching ratio. Wang [8] pointed out that, without loss of generality, the impermeability condition $f(0) + g(0) = 0$ can be replaced by $f(0) = g(0) = 0$. In the limit as $\alpha \to 0$, this bidirectional stretching sheet problem degenerates to the unidirectional stretching sheet problem solved analytically by Crane [2], i.e. $f = 1 - e^{-\eta}$ and $g = 0$.

The temperature field adjacent to the bidirectional stretching sheet is governed by the thermal boundary layer equation:

$$u\frac{\partial T}{\partial x} + v\frac{\partial T}{\partial y} + w\frac{\partial T}{\partial z} = \kappa\frac{\partial^2 T}{\partial z^2} + \frac{q}{\rho c_p}(T - T_\infty), \tag{7}$$

where the last term represents a temperature-dependent heat source ($q > 0$) or sink ($q < 0$). Laha et al. [10] considered the same problem with $q = 0$. They studied both isothermal sheets, i.e. with uniform temperature, and sheets with a uniform heat flux. In the present investigation, either the temperature or the heat flux is allowed to vary with the distance from the origin as

$$(i)\text{PST case}: T = T_w(x,y) = T_\infty + Ax^r y^s \text{ at } z = 0,$$
$$T \to T_\infty \text{ as } z \to \infty \tag{8}$$

$$(ii)\text{PHF case}: -\lambda\frac{\partial T}{\partial z} = Bx^r y^s \text{ at } z = 0,\ T \to T_\infty \text{ as } z \to \infty, \tag{9}$$

where λ is thermal conductivity of the fluid, T_∞ is the constant temperature outside the thermal boundary layer, and A and B are positive constants. The power indices r and s determine how the temperature or the heat flux at the sheet varies in the (x,y)-plane. The thermal boundary conditions (8) and (9) are by far more general than those used by Laha et al. [10]. In fact, their isothermal and uniform heat flux boundary conditions are obtained as special cases of (8) and (9), respectively, if $r = s = 0$.

For the PST case, we introduce the dimensionless temperature

$$\theta(\eta) = \frac{T(x,y,z) - T_\infty}{T_w(x,y) - T_\infty}, \tag{10}$$

which transforms the thermal energy Eq. (7) into

$$\theta'' + Pr(f+g)\theta' + Pr(\beta - rf' - sg')\theta = 0, \tag{11}$$

subjected to

$$\theta(0) = 1, \theta(\infty) = 0, \tag{12}$$

where $Pr = \upsilon/\kappa$ is the Prandtl number and $\beta \equiv q/\rho c_p a$ is the internal heat parameter. For the PHF case, the local temperature $T(x,y,z)$ relates to the dimensionless temperature $\phi(\eta)$ as

$$T(x,y,z) - T_\infty = \frac{B}{\lambda}\sqrt{\frac{\upsilon}{a}}x^r y^s \phi(\eta). \tag{13}$$

The thermal boundary layer equation remains exactly as before, i.e. with ϕ replacing θ in Eq. (11), as pointed out by Laha et al. [10]. The corresponding boundary conditions are different, however, namely

$$\phi'(0) = -1, \phi(\infty) = 0. \tag{14}$$

3. Some special cases

The hydrodynamic part of the present problem is independent of the accompanying thermal problem. The three-dimensional boundary layer problem was first formulated and solved numerically by Wang [8], whereas Ariel [9] reconsidered the same problem and derived accurate series solutions. Let us only briefly recall that the bidirectional problem considered by Wang [8] reduces to the unidirectional stretching problem due to Crane [2] for $\alpha = 0$. Wang observed that both f and f' were reduced with gradually increasing stretching rate ratio α, whereas $|f''(0)|$ increased due to the thinning of the momentum boundary layer. In spite of the reduction of $f(\infty)$ with increasing α, the sum $f(\infty) + g(\infty)$ tended to increase monotonically from 1.0 for $\alpha = 0$ to 1.50305 for $\alpha = 1$. This essential observation, which was not addressed by Wang [8], implies that the ambient flow rate entrained perpendicular towards the sheet is about 50% higher with axisymmetric stretching ($\alpha = 1$) than with unidirectional stretching ($\alpha = 0$).

3.1. Special case $\alpha = 0$

In the case of unidirectional stretching, the fluid motion is solely in the (x,z)-plane, i.e. g and g' in Eq. (1) are both

zero. This special case is equivalent with the heat transfer problem considered by Carragher and Crane [6] and Grubka and Bobba [7], in which the temperature difference between the sheet and its surroundings was proportional to a power of the distance from the slit through which the sheet emerged. The temperature field can be expressed in terms of confluent hypergeometric functions ${}_1F_1(m; n; x)$

$$(\mathrm{PST})\theta(\eta) = \mathrm{e}^{-(m+n)\eta}\frac{{}_1F_1(m+n-r;1+2n;-Pr\mathrm{e}^{-\eta})}{{}_1F_1(m+n-r;1+2n;-Pr)}, \quad (15)$$

where $m = Pr/2$ and $n = \sqrt{Pr^2 - 4\beta Pr}/2$. Similarly, the solution for the corresponding case in which the heat flux at the sheet exhibits a power-law variation in x becomes

$$(\mathrm{PHF})\phi(\eta) = \mathrm{e}^{-(m+n)\eta}{}_1F_1(m+n-r;1+2n;-Pr\mathrm{e}^{-\eta})/C \quad (16)$$

where the constant denominator is given as

$$C = \left[(m+n){}_1F_1(m+n-r;1+2n;-Pr) - Pr\frac{m+n-r}{1+2n}{}_1F_1(m+n-r+1;2+2n;-Pr)\right].$$

3.2. Special case r = s = 0 and β = 0

With both r and s equal to zero and $\beta = 0$ (no heat source or sink), the thermal surface conditions defined in Eqs. (8) and (9) simplify to $T_w = T_\infty + A$ and $-\lambda\partial T/\partial z = B$, respectively, i.e. constant surface temperature and constant surface heat flux. This is identical to the thermal boundary layer problem studied by Laha et al. [10]. They presented numerical solutions of this two-parameter problem for some different values of the stretching ratio in the range $0 \leqslant \alpha \leqslant 1$. Their results for the lowest Prandtl number considered ($Pr = 0.1$) are, however, not reliable since they used a by far too short integration domain in view of the excessive thickening of thermal boundary layers at low Prandtl numbers.

3.3. Special case α = 1, β = 0 and Pr = 1

Wang [8] observed that the flow is axisymmetric when $\alpha = 1$, i.e. when the stretching rate is the same in the x- and y-directions. This implies that $f(\eta) = g(\eta)$ and the hydromechanical problem (2)–(6) simplifies considerably. In this case, it can also be shown that the solution $f'(\eta)$ for the lateral fluid velocity also solves the thermal energy Eq. (11) subject to the boundary conditions (12) if $\beta = 0$, $Pr = 1$, and $r + s = 1$. This implies that the numerical solution of the hydrodynamic problem for $\alpha = 1$ is also a solution of the temperature field for this particular parameter combination. It is particularly noteworthy that only the sum $r + s$ matters and not the individual values of r and s.

4. Numerical method

The ODE (11) subject to either Eq. (12) or Eq. (13) forms a two-point boundary value problem (BVP) on the semi-infinite domain $[0, \infty)$ in the four independent parameters Pr, r, s, and β. To the authors' knowledge, closed-form solutions for the dimensionless temperature profiles $\theta(\eta)$ and $\phi(\eta)$ are not available. We therefore resort to numerical integration. The entire BVP, i.e. including the hydrodynamic part, consists of eight first-order ODEs with five boundary conditions (BCs) at the stretching surface and three at infinity. For the PST case Eqs. (4), (5) and (11) are first integrated numerically using a fifth-order Runge–Kutta scheme from zero to infinity with five prescribed values $f(0) = g(0) = f'(0) - 1 = g'(0) - \alpha = \theta(0) - 1 = 0$ and three trial values $f''(0)$, $g''(0)$ and $\theta'(0)$. In the PHF case, the five prescribed boundary conditions are $f(0) = g(0) = f'(0) - 1 = g'(0) - \alpha = \phi'(0) + 1 = 0$, whereas the three guessed values become $f''(0)$, $g''(0)$ and $\phi(0)$. With arbitrary trial values, however, the integrated solutions will in general not satisfy the far-field boundary conditions $f'(\infty) = 0$, $g'(\infty) = 0$ and either $\theta(\infty) = 0$ or $\phi(\infty) = 0$ for the PST and the PHF case, respectively. To this end a Newton–Raphson based scheme is employed to adjust the three trial values such that the integrated solutions eventually match the required far-field boundary conditions. The Newton–Raphson process is continued until the sum of the squared errors at the far-field boundary is lower than 10^{-12}. Wang [8] found that it was sufficient to integrate the ODEs of the hydrodynamic part of the BVP up to a maximum value of $\eta_\infty = 10$. Since the thickness of the thermal boundary layer roughly varies inversely with the

Table 1
Numerical results of the hydrodynamical problem

		$f''(0)$	$g''(0)$	$f(\infty)$	$g(\infty)$
Wang [8]	$\alpha = 0$	−1	0	1	0
Present study		−1	0	1	0
Wang [8]	$\alpha = 0.25$	−1.048813	−0.194564	0.907075	0.257986
Present study		−1.048813	−0.194565	0.907067	0.257966
Wang [8]	$\alpha = 0.5$	−1.093097	−0.465205	0.842360	0.451671
Present study		−1.093096	−0.465206	0.842361	0.451663
Wang [8]	$\alpha = 0.75$	−1.134485	−0.794622	0.792308	0.612049
Present study		−1.134486	−0.794619	0.792293	0.612128
Wang [8]	$\alpha = 1$	−1.173720	−1.173720	0.751527	0.751527
Present study		−1.173721	−1.173721	0.751494	0.751494

Present results are compared with data from Table 1 in Wang [8].

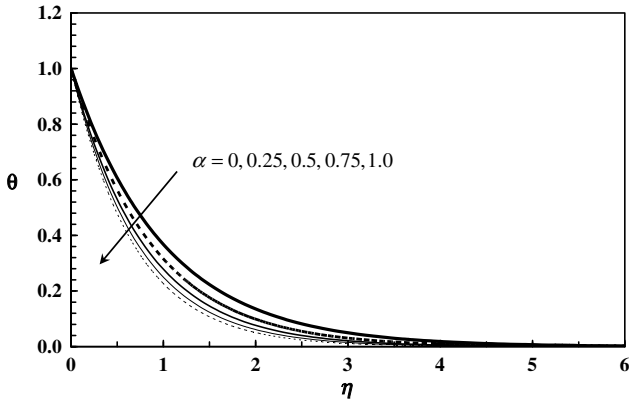

Fig. 2. Temperature profiles $\theta(\eta)$ for selected values of the stretching rate ratio α for $Pr = 1$, $r = 1$, $s = 1$ and $\beta = 0$.

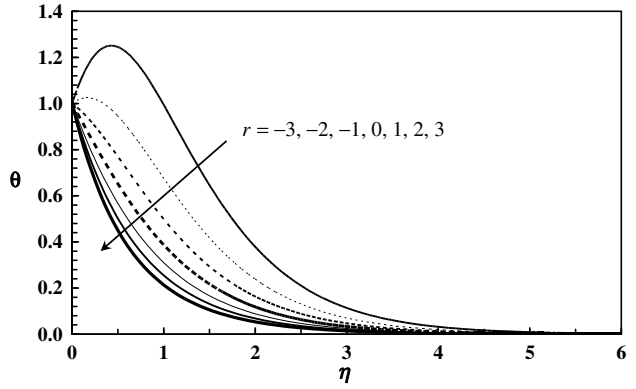

Fig. 3a. PST: Temperature profile $\theta(\eta)$ for selected r with $Pr = 1$, $\alpha = 0.5$, $s = 0$ and $\beta = 0$.

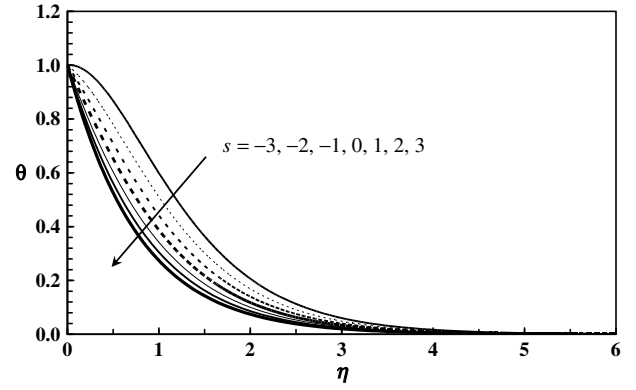

Fig. 3b. PST: Temperature profiles $\theta(\eta)$ for selected s with $Pr = 1$, $\alpha = 0.5$, $r = 0$ and $\beta = 0$.

square root of Pr, a substantially larger integration domain is required at the lowest Prandtl numbers. To demonstrate the accuracy of the integration scheme, the present results are compared with data from Wang [8] in Table 1.

5. Results and discussion

The present investigation is concerned with the heat transfer characteristics accompanying the three-dimensional flow and in particular the influence of non-uniform sheet conditions (represented herein by the power indices r and s) and the potential role of a heat source or sink ($\beta \neq 0$). Let us first, however, examine how the stretching ratio α, i.e. the only hydrodynamic parameter, affects the thermal boundary layer for a specific combination of the four thermal parameters Pr, r, s, and β. The dimensionless temperature profiles $\theta(\eta)$ presented in Fig. 2 show that the temperature decreases with increasing values of the stretching ratio α. These results are in qualitative agreement with the temperature profiles shown by Laha et al. [10] for an isothermal sheet ($r = s = 0$) for $Pr = 0.5$ and with $\beta = 0$. The observed thinning of the thermal boundary layer with higher values of α is a consequence of the higher entrainment of cooler fluid from the ambient.

The power indices r and s control the non-uniformity of the sheet temperature in the prescribed sheet temperature case. The temperature profiles in Fig. 3a show the effect of r for given s ($s = 0$), while Fig. 3b shows how s affects the temperature when the sheet temperature is uniform in the x-direction ($r = 0$). It is readily observed that the non-uniformity of the sheet temperature has a significant influence on the temperature profiles and both increasing r and s values tend to reduce the temperature and make the thermal boundary layer thinner. The temperature profiles computed by Grubka and Bobba [7] for unidirectional stretching with a power-law variation of the sheet temperature and $Pr = 0.72$ show exactly the same behavior as the present results in Fig. 3a for a bidirectional stretching sheet with a prescribed sheet temperature which varies as x^r but is independent of y.

It is noteworthy that the present results for bidirectional stretching $\alpha = 0.5$ show a more pronounced influence of r than of s. This is not at all surprising since r and s contribute to the term $-Pr(rf' + sg')\ \theta$ in the thermal boundary layer Eq. (11) and f' is roughly twice as large as g' for this particular α-value. From Fig. 3a we observe that the temperature rises above the sheet temperature T_w before it decays to the ambient temperature T_∞ for $r = -3$ and $r = -2$. In these cases the sheet temperature becomes lower

Table 2
Temperature gradient at the surface $\theta'(0)$ for selected values of r, s and α with $Pr = 1$ and $\beta = 0$

Stretching ratio	$r = 0$, $s = 0$	$r = -2$, $s = 0$	$r = 2$, $s = 0$	$r = 0$, $s = -2$	$r = 0$, $s = 2$
$\alpha = 0.25$	−0.665933	0.554512	−1.364890	−0.413111	−0.883125
$\alpha = 0.5$	−0.735334	0.308578	−1.395356	−0.263381	−1.106491
$\alpha = 0.75$	−0.796472	0.135471	−1.425038	−0.126679	−1.292003

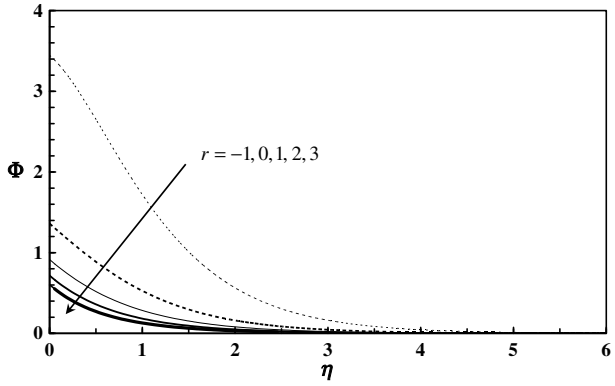

Fig. 4a. PHF: Temperature profiles $\phi(\eta)$ for selected r with $Pr = 1$, $\alpha = 0.5$, $s = 0$ and $\beta = 0$.

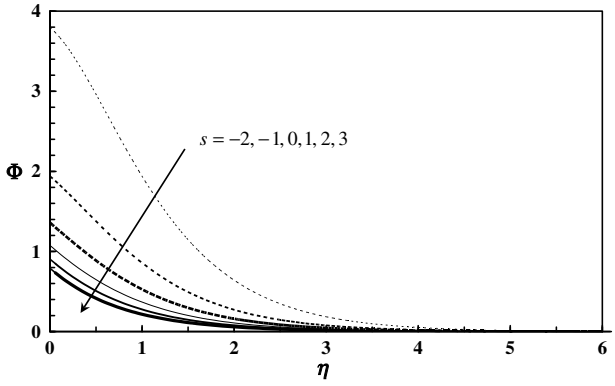

Fig. 4b. PHF: Temperature profiles $\phi(\eta)$ for selected s with $Pr = 1$, $\alpha = 0.5$, $r = 0$ and $\beta = 0$.

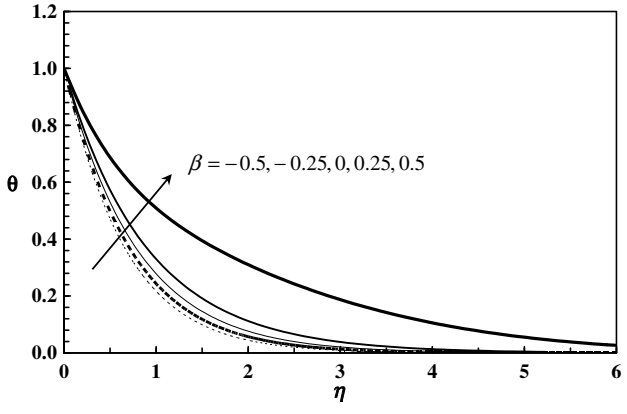

Fig. 5. Temperature profiles $\theta(\eta)$ for selected β with $Pr = 1$, $\alpha = 0.5$, $r = 1$ and $s = 1$.

as the distance x from the origin increases and the heat flux is therefore directed from the fluid to the sheet, rather than in the common direction from the sheet to the fluid (as for r-values >-1). This peculiar phenomenon can be explained by means of the governing ODE (11) with $\beta = 0$. Let us set $r = s = -1$ and integrate the equation once after a slight rearrangement of the terms. By use of the boundary conditions (12) and the auxiliary requirement that θ' should vanish as $\eta \to \infty$, we arrive at the following integral:

$$\theta' + Pr(f + g)\theta = 0 \tag{17}$$

which is valid for arbitrary values of the stretching ratio α. Since $f(0)$ and $g(0)$ both vanish at the sheet, Eq. (17) implies that $\theta'(0) = 0$. Physically this means that if the sheet temperature varies as $T_w = T_\infty + Ax^{-1}y^{-1}$, there is no heat transfer between the sheet and the fluid. Results for the temperature gradient at the sheet $\theta'(0)$ are provided in Table 2. Only for the parameter combination $r = -2$ and $s = 0$ is the heat flow from the fluid towards the sheet, i.e. $\theta'(0) > 0$. We have already shown that $\theta'(0) = 0$ if $r = s = -1$. Since $f' > g'$ for all values of $\alpha \leqslant 1$, the temperature gradient $\theta'(0)$ becomes positive for $r = -2$ and $s = 0$ and negative for $r = 0$ and $s = -2$.

Some sample results for the case with prescribed heat transfer at the sheet are shown in Fig. 4. Here, the temperature and, in particular, the sheet temperature $\phi(0)$ decrease with r and s. Inspection of Eq. (11) shows that $\phi''(0) = 0$ if $r = s = 0$. Thus, the temperature profiles in Fig. 4a exhibit an inflection point for $r < 0$ and the profiles in Fig. 4b similarly exhibit an inflection point for negative s-values. In these cases the largest temperature gradient is not at the sheet but somewhat above the surface. It might be interesting to observe that although the integrated thermal energy Eq. (17) is formally valid also in the PHT case, no solution exist which satisfies the boundary condition $\phi'(0) = -1$. This proves the non-existence of solutions for the prescribed heat flux case for $r = s = -1$.

Finally, the influence of a heat source or sink on the temperature field is illustrated in Fig. 5, which shows temperature profiles calculated for the same stretching ratio α as in Figs. 3 and 4 and for a specific combination of the thermal parameters. As expected, the temperature rises with increasing source strength $\beta > 0$ whereas a heat sink $\beta < 0$ tends to lower the temperature. The data provided in Table 3 show that the heat transfer rate $-\theta'(0)$ reduces with increasing β-values. This is a direct consequence of the thickening of the thermal boundary layer with β and the results in Table 3 suggest that this effect prevails for

Table 3
$\theta'(0)$ and $\phi(0)$ for selected values of β and Pr with $\alpha = 0.5$, $r = 1$ and $s = 1$

	$\theta'(0)$ for PST			$\phi(0)$ for PHF		
	$\beta = -0.2$	$\beta = 0$	$\beta = 0.2$	$\beta = -0.2$	$\beta = 0$	$\beta = 0.2$
$Pr = 1$	−1.348064	−1.255781	−1.148932	0.741805	0.796317	0.870355
$Pr = 5$	−3.33039	−3.170979	−3.002380	0.300265	0.315360	0.333069
$Pr = 10$	−4.812149	−4.597141	−4.371512	0.207807	0.217527	0.228754

all Prandtl numbers. In cases with prescribed heat flux at the sheet, a heat source (sink) tends to enhance (reduce) the sheet temperature $\phi(0)$.

6. Concluding remarks

The steady three-dimensional thermal boundary layer along a bidirectional stretching surface has been studied. Two different cases have been considered: (i) prescribed surface temperature and (ii) prescribed surface heat flux. The focus of the investigation has been on the effects of variable surface conditions. The present work is therefore a generalization of the earlier study by Laha et al. [10] who considered uniform thermal conditions at the surface. In addition, the present analysis also includes an internal heat source or sink.

It has been observed that the variation of the sheet temperature has a substantial effect on the thermal boundary layer. This effect is most pronounced when sheet temperature varies in the direction of the highest stretching rate. If the temperature decreases along the direction of stretching, the location of maximum temperature may even be offset from the surface. When the heat transfer rate at the surface varies in the lateral directions, the resulting sheet temperature is substantially affected.

References

[1] B.C. Sakiadis, Boundary-layer behavior on continuous solid surfaces: I. Boundary-layer equations for two-dimensional and axisymmetric flow, AIChE. J. 7 (1961) 26–28.
[2] L.J. Crane, Flow past a stretching plate, ZAMP 21 (1970) 645–647.
[3] P.S. Gupta, A.S. Gupta, Heat and mass transfer on a stretching sheet with suction or blowing, Can. J. Chem. Eng. 55 (1977) 744–746.
[4] J. Vleggaar, Laminar boundary-layer behaviour on continuous accelerating surfaces, Chem. Eng. Sci. 32 (1977) 1517–1525.
[5] B.K. Dutta, P. Roy, A.S. Gupta, Temperature field in flow over a stretching sheet with uniform heat flux, Int. Commun. Heat Mass Transfer 12 (1985) 89–94.
[6] P. Carragher, L.J. Crane, Heat transfer on a continuous stretching sheet, Z. Angew. Math. Mech. 62 (1982) 564–565.
[7] L.J. Grubka, K.M. Bobba, Heat transfer characteristics of a continuous stretching surface with variable temperature, ASME J. Heat Transfer 107 (1985) 248–250.
[8] C.Y. Wang, The three-dimensional flow due to a stretching surface, Phys. Fluids 27 (1984) 1915–1917.
[9] P.D. Ariel, Generalized three-dimensional flow due to a stretching sheet, Z. Angew. Math. Mech. 83 (2003) 844–852.
[10] M.K. Laha, P.S. Gupta, A.S. Gupta, Heat transfer characteristics of the flow of an incompressible viscous fluid over a stretching sheet, Wärme Stoffübertrag. 24 (1989) 151–153.